Research Square

Preprints are preliminary reports that have not undergone peer review.
They should not be considered conclusive, used to inform clinical practice,
or referenced by the media as validated information.

Exploring E-3-alkenyl 1,2,4- and 1,3,4-Oxadiazoles as Electrophilic Warheads: Synthesis and Evaluation of Novel Michael Acceptors Targeting Thioredoxin Reductase for Cancer Treatment

Anton A. Shetnev

a.shetnev@list.ru

Yaroslavl State Pedagogical University

Marina V. Tarasenko

Yaroslavl State Pedagogical University

Valentina D. Kotlyarova

Yaroslavl State Pedagogical University

Alexander M. Silin

Yaroslavl State Pedagogical University

Mikhail G. Mikhalsky

Russia Institute of Chemistry, Saint Petersburg State University

Alexandrina S. Volobueva

Russia Institute of Chemistry, Saint Petersburg State University

Eugenii G. Chupakhin

Immanuel Kant Baltic Federal University Institute of Chemistry, Saint Petersburg State University, Universitetskaya Nab

Sergey V. Baykov

Russia Institute of Chemistry, Saint Petersburg State University

---

Research Article

Keywords: heterocycles; oxadiazole; thioredoxin reductase, cytotoxity, Michael acceptor, anticancer agents

Posted Date: November 26th, 2026

DOI: https://doi.org/10.21203/rs.3.rs-11672391/v1

License: This work is licensed under a Creative Commons Attribution 4.0 International License.
Read Full License

Additional Declarations: No competing interests reported.

Abstract

A series of twelve novel Michael acceptors based on 1,2,4- and 1,3,4-oxadiazole scaffolds bearing acrylic acid moieties was designed, synthesized, and evaluated as potential inhibitors of thioredoxin reductase 1 (TrxR1). 1,2,4-Oxadiazole derivatives were prepared via a one-pot O-acylation/heterocyclization/retro-Diels–Alder sequence, while 1,3,4-oxadiazole analogues were obtained by cyclodehydration of maleamic acid intermediates. Biological evaluation revealed that six compounds significantly inhibited TrxR1 in SH-SY5Y cell lysate at 25 μM. Compound **7b** was the most potent inhibitor of recombinant rat TrxR1 (IC_{50} = 6.0 μM), followed by **7a** (15.8 μM), **3g** (19.7 μM), and **3f** (27.0 μM). However, despite effective enzymatic inhibition, all compounds exhibited weak cytotoxicity against H23 and HeLa cancer cell lines in comparison with oxaliplatin, indicating a discrepancy between enzymatic and cellular activity. This observation suggests limitations in membrane permeability, intracellular accumulation, or compensatory redox mechanisms.

Introduction

Thioredoxin reductase (TrxR) is a selenium-dependent dimeric flavoprotein that, together with thioredoxin (Trx) and NADPH, constitutes a central system for maintaining cellular redox homeostasis [1]. Elevated TrxR expression is observed in a wide range of malignant tumours and correlates with aggressive disease progression, poor prognosis, and resistance to conventional chemotherapy [1]. Inhibition of TrxR leads to accumulation of reactive oxygen species (ROS), disruption of deoxyribonucleotide biosynthesis, and activation of caspase-dependent cell death pathways in cancer cells, rendering selective TrxR inhibitors a promising alternative to traditional chemotherapeutic agents [2].

Among the most clinically advanced candidates are auranofin (currently under repurposing for oncological indications and having shown activity in several Phase II trials), ethaselen (Phase II), and PX-12 (which completed Phase II studies but was not further advanced). A particularly attractive strategy involves the design of bifunctional molecules that simultaneously inhibit TrxR and generate ROS, thereby overcoming the adaptive resilience of the antioxidant network in cancer cells.

Design approaches for TrxR inhibitors can be classified according to their mechanism of interaction with the enzyme active site: substrate-like inhibitors (typically selenium-containing electrophilic heterocycles), irreversible inhibitors, and reversible inhibitors based on natural or synthetic heterocyclic Michael acceptors [3]. Heterocyclic compounds occupy a central position among the TrxR inhibitors studied to date, owing to their structural diversity, the feasibility of fine-tuning their physicochemical properties, and their ability to engage in covalent or non-covalent interactions with the selenol moiety of Sec498 [4–15].

In current medicinal chemistry, 1,3,4- and 1,2,4-oxadiazole heterocycles have attracted considerable interest, having proven themselves as valuable pharmacophoric motifs in antimicrobial, antiviral, anti-inflammatory, and anticancer agents [23]. The introduction of an unsaturated alkenyl functionality at the heterocyclic periphery offers the opportunity to design ligands capable of forming covalent bonds via

Michael addition with selenocysteine residues, as well as engaging in specific π–stacking interactions with aromatic amino acid residues in the TrxR active site. Nevertheless, systematic structure–activity relationship (SAR) studies for alkenyloxadiazoles with respect to TrxR1 inhibition have not been reported to date. Accordingly, this article presents the rational design, efficient synthesis, and comprehensive biological evaluation of alkenyloxadiazoles as potential TrxR1 inhibitors discusses their prospects as core scaffolds for the development of next-generation therapeutics.

Results and discussion

Chemistry

Inspired by the results obtained for the amide-containing Michael acceptor DVD-445, we proposed the design of a new chemotype of Michael acceptors based on oxadiazole-containing acrylic acids and their derivatives [16].

To test this hypothesis, a series of ten (E)-1,2,4-oxadiazol-5-ylacrylic acids bearing various substituents was synthesized using our previously developed original approach, which relies on the reaction of commercially and synthetically readily available amidoximes with *exo*-3,6-epoxy-1,2,3,6-tetrahydrophthalic anhydride. The method involved a one-pot sequence comprising O-acylation of the amidoximes with *exo*-3,6-epoxy-1,2,3,6-tetrahydrophthalic anhydride, followed by heterocyclization of the resulting O-acylamidoximes under superbasic conditions, and a final acid-catalysed retro-Diels–Alder reaction. This stereoselective protocol afforded the substituted (E)-1,2,4-oxadiazol-5-ylacrylic acids in good to moderate yields, bearing diverse substituents on the aryl moiety [17].

Scheme 1. Synthetic route to (*E*)-1,2,4-oxadiazol-5-yl-acrylic acids.

Furthermore, employing a scaffold-hopping strategy, we replaced the 1,2,4-oxadiazole core with the 1,3,4-oxadiazole moiety. The resulting 1,3,4-oxadiazol-5-ylacrylic acids were obtained via a two-step procedure involving the reaction of hydrazides with maleic anhydride in acetic acid. The product from the first step, isolated by filtration, was subsequently subjected to cyclodehydration using phosphorus oxychloride in DMF under cooling. The final products were obtained as mixtures of *cis* and *trans* isomers of the substituted acrylic acids, which were then separated by crystallization (Scheme 2) according to literature procedures [18, 19].

Scheme 2. Synthetic routes to 1,3,4-oxadiazol-5-ylacrylic acids and the final compound library.

As a result, two analogues of the 1,2,4-oxadiazole series bearing a methyl substituent at the 2-position and a 4-nitro substituent were obtained.

Overall, a compound library of twelve Michael acceptor derivatives was obtained for biological evaluation (Scheme 2).

Results of In Vitro Biological Studies

A series of twelve novel Michael acceptors (oxadiazol-5-yl acrylic acids) was evaluated for TrxR1 inhibitory activity. Compounds **3a–l**, along with compounds **7a** and **7b**, were tested for their ability to inhibit TrxR activity using an assay based on human neuroblastoma (SH-SY5Y) cell lysate. Piperlongumine [22] was employed as a positive control. The TrxR activity assay with cell lysate is a kinetic assay in which the total protein content of the cells is assessed colorimetrically using 5,5'-dithiobis(2-nitrobenzoic acid) (DTNB, Ellman's reagent) as a substrate.

To our delight, six of the twelve compounds tested (**3b**, **3e**, **3f**, **3g**, and, notably, **7a** and **7b**) displayed significant inhibition of TrxR activity in SH-SY5Y cell lysate at 25 μM (Fig. 1). Based on the inhibitory potential observed in the cell lysate assay, IC_{50} values were determined for four inhibitors (**3f**, **3g**, **7a**, and **7b**). Their activity was further evaluated in a colorimetric DTNB assay against recombinant rat TrxR1. One compound (**7b**) demonstrated strong inhibition of rat TrxR1, with an IC_{50} value of 6.0 μM. The remaining active compounds exhibited the following IC_{50} values against rat TrxR1: **3f**, 27.0 ± 1.0 μM; **3g**, 19.7 ± 3.0 μM; and **7a**, 15.8 ± 2.7 μM (Fig. 2, Table 1).

The cytotoxicity of compounds **3a–l**, **7a–b** was investigated against human lung adenocarcinoma cell line H23 and human cervical adenocarcinoma cell line HeLa, using the MTT assay with oxaliplatin as a positive control. Relevant cytotoxicity data set for previously identified most active TrxR1 inhibitors and its amide derivatives were summarized in Table 1.

Table 1
Cytotoxicity of hit-compounds **3f**, **3g**, **7a**, **7b** in H23 and HeLa cell lines at 72 h incubation time

Compound	**TrxR Assay (SH-SY5Y lysate)**	**Cytotoxicity Assay**	
	IC_{50}, μM	**IC_{50}, μM**	
		H23	**HeLa**
3f	27.0 ± 1.0	94.5 ± 7.6	125.6 ± 11.3
3g	19.7 ± 3.0	103.5 ± 10.4	154.3 ± 18.5
7a	15.8 ± 2.7	987.3 ± 167.8	900.1 ± 108.1
7b	6.0 ± 1.0	794.3 ± 63.5	251.5 ± 17.6
Oxaliplatin	-	56.1 ± 9.5	6.4 ± 0.7
Piperlongumine	46 ± 6	-	-

Over a concentration range 1-1000 μM and incubation period of 72 h, the tested compounds exhibit different cytotoxicity effects with compound **3g** being the most promising candidate. Clearly, this preliminary cytotoxicity assessment should be complemented by further studies evaluating these compounds as adjuvant agents in combination with systemic and targeted cytostatic drugs.

Molecular Docking Studies

We performed covalent docking of 12 oxadiazole Michael acceptors to rat thioredoxin reductase 1 (TrxR1) to model their adduct poses at the catalytic selenocysteine residue Sec498. The starting model was the crystal structure of the enzyme with a reduced C-terminal tail (PDB ID 3EAN) [30].

The estimated binding energies were compared with absorbance at 412 nm measured 20 min after DTNB addition in SH-SY5Y cell lysate at a compound concentration of 25 μM (Table 2). The rankings showed partial agreement across the 12 compounds (Spearman's ρ = 0.49). Compounds **7b** and **7a** gave the lowest A_{412} values (0.21 and 0.22, respectively). Compound **3j** had one of the most negative estimated binding energies (− 4.622 kcal/mol), although its endpoint absorbance was the same as that of the control without added compound (0.52).

In the modeled pose of the **7b** adduct, a nitrogen atom of the oxadiazole ring forms a hydrogen bond with Gln494, and the carboxylic acid group forms two hydrogen bonds with Gly499. The aryl group makes hydrophobic contacts with Val484 and Ile492 (Fig. 3).

Table 2
Endpoint absorbance in the DTNB assay and estimated binding energies (COOH/β-R).

Compound	A_{412} at 20 min	Estimated binding energy, (kcal/mol)
3g	0.30	−4.567
3f	0.33	−4.672
3c	0.41	−4.568
3b	0.42	−4.454
3a	0.49	−4.325
3d	0.50	−3.830
3e	0.51	−4.350
3j	0.52	−4.622
3k	0.52	−3.873
3l	0.52	−4.147
7b	0.21	−4.621
7a	0.22	−4.417

The compound concentration was 25 μM. The control without added compound had an endpoint absorbance of 0.52. Spearman's ρ was calculated across the 12 compounds using average ranks for

ties.

Conclusion

In summary, we have designed and synthesized a focused library of sixteen oxadiazole-based Michael acceptors, including both 1,2,4- and 1,3,4-oxadiazole scaffolds. Biological evaluation identified compound **7b** as a potent inhibitor of recombinant rat TrxR1 (IC_{50} = 6.0 μM) and compounds **3f**, **3g**, and **7a** as moderate inhibitors (IC_{50} = 15.8–27.0 μM). However, despite significant enzymatic inhibition, all tested compounds exhibited weak cytotoxicity against H23 and HeLa cancer cell lines, suggesting that optimization of cellular uptake and/or evaluation in combination regimens is required to realize their therapeutic potential.

These findings provide a foundation for further structural optimization aimed at improving membrane permeability and intracellular accumulation of oxadiazole-based TrxR1 inhibitors, as well as for exploring their potential as adjuvants in combination cancer therapy.

Experimental section

General

All reagents and solvents were obtained from commercial source (Acros, Merck) and used without additional purification. All other reagents and solvents were purchased and used without further purification. Reactions were monitored by analytical thin layer chromatography (TLC) Macherey-Nagel, TLC plates SiliaPlate TLA-R10011B-323 using UV light for detection. Column chromatography was carried out with silica gel grade 60 (0.040–0.063 mm) 230–400 mesh with a hexane–ethyl acetate mixture as eluent. NMR spectra were recorded on BrukerAVANCE DPX 400 (at 400 MHz and 101 MHz for ^{1}H and ^{13}C respectively). Chemical shifts are reported as parts per million (δ, ppm); the residual solvent peaks were used as internal standards: 7.26 and 2.50 ppm for ^{1}H in $CDCl_3$ and DMSO-d_6 respectively, 39.52 and 77.16 ppm for ^{13}C in DMSO-d_6 and $CDCl_3$ respectively; multiplicities are abbreviated as follows: s = singlet, d = doublet, t = triplet, q = quartet, m = multiplet, br = broad; coupling constants, *J*, are reported in Hertz (Hz). Melting points were determined in open capillary tubes on Electrothermal IA 9300 series Digital Melting Point Apparatus. High-resolution mass spectra (HRMS) were measured on Bruker maXis HRMSESI-QTOF (ESI Ionization).

Starting amidoximes **1a-l** were synthesized by reaction of commercial nitriles with hydroxylamine hydrochloride [24].

Synthetic Work

Synthesis and Characterization of 1,2,4-Oxadiazol-5-ylacrylic Acids (3a–l)

General procedure. To a solution of amidoxime **1** (1 mmol) in dry DMSO (1 mL) was added *exo*-3,6-epoxy-1,2,3,6-tetrahydrophthalic anhydride **2** (182 mg, 1.1 mmol), and the reaction mixture was stirred at room temperature for 20 h. Then powdered NaOH (92 mg, 2.3 mmol) was added rapidly. After the addition, the reaction mixture was stirred at room temperature for 1 h. The mixture was then diluted with CF_3COOH (1 mL) and stirred at 60–70°C for 1 h. After cooling to room temperature, the mixture was diluted with cold water (5 mL). The precipitated solid was filtered off, washed with cold water (2 × 2 mL), and dried in air at 50°C. The crude product was recrystallized from Et_2O or purified by column chromatography on silica gel using CH_2Cl_2/MeOH (1:0.05) as eluent.

(E)-3-(3-(5-Methylthiophen-2-yl)-1,2,4-oxadiazol-5-yl)acrylic acid (3a) [17]

White powder; 62% yield (146 mg); mp 163–164°C. ^{1}H NMR (400 MHz, DMSO-d_6): δ 13.38 (s, 1H), 7.66 (d, *J* = 3.6 Hz, 1H), 7.45 (d, *J* = 16.1 Hz, 1H), 7.02–6.97 (m, 2H), 2.55 (s, 3H).

(E)-3-(3-(p-Tolyl)-1,2,4-oxadiazol-5-yl)acrylic acid (3b) [17]

White powder; 79% yield (182 mg); mp 185–187°C. ^{1}H NMR (400 MHz, $CDCl_3$): δ 7.89 (d, *J* = 8.2 Hz, 2H), 7.40 (dd, *J* = 16.0, 2.2 Hz, 1H), 7.24 (d, *J* = 8.0 Hz, 2H), 6.96 (dd, *J* = 16.0, 2.2 Hz, 1H), 2.34 (s, 3H).

(E)-3-(3-(Benzo[d][1, 3]**dioxol-5-yl)-1,2,4-oxadiazol-5-yl)acrylic acid (3c)** [17]

White powder; 53% yield (138 mg); mp 220–222°C. ^{1}H NMR (400 MHz, DMSO-d_6): δ 13.32 (br s, 1H), 7.60 (d, *J* = 8.1 Hz, 1H), 7.51–7.41 (m, 2H), 7.11 (d, *J* = 8.1 Hz, 1H), 7.00 (d, *J* = 16.2 Hz, 1H), 6.15 (s, 2H).

(E)-3-(3-(Thiophen-3-yl)-1,2,4-oxadiazol-5-yl)acrylic acid (3d)[17]

White powder; 52% yield (116 mg); mp 189–191°C.^{1}H NMR (400 MHz, DMSO-d_6): δ 13.38 (s, 1H), 8.37–8.33 (m, 1H), 7.81 (dd, *J* = 4.8, 3.0 Hz, 1H), 7.62 (d, *J* = 4.7 Hz, 1H), 7.48 (d, *J* = 16.1 Hz, 1H), 7.02 (d, *J* = 16.1 Hz, 1H).

(E)-3-(3-(3,5-Dichlorophenyl)-1,2,4-oxadiazol-5-yl)acrylic acid (3e) []

White powder; 70% yield (198 mg); mp 246–249°C. ^{1}H NMR (400 MHz, DMSO-d_6): δ 13.46 (s, 1H), 8.00 (s, 2H), 7.93 (s, 1H), 7.51 (d, *J* = 16.1 Hz, 1H), 7.07 (d, *J* = 16.1 Hz, 1H).

(E)-3-(3-(o-Tolyl)-1,2,4-oxadiazol-5-yl)acrylic acid (3f) [17]

White powder; 69% yield (159 mg); mp 161–162°C. ^{1}H NMR (400 MHz, DMSO-d_6): δ 13.35 (s, 1H), 7.96–7.93 (m, 1H), 7.53–7.47 (m, 2H), 7.41 (dd, *J* = 15.7, 7.6 Hz, 2H), 7.03 (d, *J* = 16.1 Hz, 1H), 2.58 (s, 3H).

(E)-3-(3-(4-Nitrophenyl)-1,2,4-oxadiazol-5-yl)acrylic acid (3g) [17]

Pale yellow powder; 63% yield (165 mg); mp 171–174°C.^{1}H NMR (400 MHz, DMSO-d_6): δ 13.37 (s, 1H), 7.99 (d, *J* = 8.6 Hz, 2H), 7.52–7.43 (m, 1H), 7.13 (d, *J* = 8.7 Hz, 2H), 7.01 (d, *J* = 16.1 Hz, 1H).

(E)-3-(3-(m-Tolyl)-1,2,4-oxadiazol-5-yl)acrylic acid (3j) [17]

White powder; 47% yield (108 mg); mp 215–219°C. ^{1}H NMR (400 MHz, DMSO-d_6): δ 13.38 (s, 1H), 7.89–7.83 (m, 2H), 7.52–7.43 (m, 3H), 7.03 (d, *J* = 16.1 Hz, 1H), 2.42 (s, 3H).

(E)-3-(3-(4-Bromophenyl)-1,2,4-oxadiazol-5-yl)acrylic acid (3k) [17]

White powder; 42% yield (124 mg); mp 208–209°C. ^{1}H NMR (400 MHz, DMSO-d_6): δ 13.39 (s, 1H), 7.98 (d, *J* = 8.2 Hz, 2H), 7.81 (d, *J* = 8.1 Hz, 2H), 7.49 (d, *J* = 16.1 Hz, 1H), 7.03 (d, *J* = 16.1 Hz, 1H).

(E)-3-(3-(2,4-Dimethoxyphenyl)-1,2,4-oxadiazol-5-yl)acrylic acid (3l) [17]

White powder; 55% yield (152 mg); mp 204–207°C. ^{1}H NMR (400 MHz, DMSO-d_6): δ 13.32 (s, 1H), 7.85 (d, *J* = 8.6 Hz, 1H), 7.46 (d, *J* = 16.1 Hz, 1H), 6.98 (d, *J* = 16.1 Hz, 1H), 6.76–6.70 (m, 2H), 3.89 (s, 3H), 3.86 (s, 3H).

Synthesis and Characterization of 1,3,4-Oxadiazol-5-ylacrylic Acids (7a, b)

1,3,4-Oxadiazol-5-yl acrylic acids **7a, b** were obtained according to a previously reported method [18]:

General procedure. To a vigorously stirred solution of maleic anhydride (108 mg, 1.1 mmol) in glacial AcOH (3 mL) was added a solution of the corresponding benzohydrazide **4a,b** (1 mmol) in glacial AcOH (3.5 mL). A precipitate formed immediately. The mixture was stirred at room temperature for 20 min. The precipitate was then filtered off, washed with glacial AcOH on the filter, and dried. A solution of the corresponding (Z)-4-(2-aroylhydrazino)-4-oxo-2-butenoic acid **6a,b** (1 mmol) in dry DMF (1 mL) was treated dropwise with $POCl_3$ (0.112 mL, 1.2 mmol) while maintaining the temperature below 40°C. The reaction mixture was stirred at room temperature for 20 min. The mixture was then poured onto ice-cold water, and a white precipitate of **7a, b** formed immediately. The precipitate was filtered off, washed with water on the filter, and dried. The crude product was recrystallized from EtOH.

(E)-3-(5-(4-Nitrophenyl)-1,3,4-oxadiazol-2-yl)acrylic acid (7a) [18].

Pale yellow powder; 80% yield (215 mg); mp 265–266°C. ^{1}H NMR (400 MHz, DMSO-d_6): δ 12.02 (s, 1H), 9.51 (d, *J* = 7.8 Hz, 1H), 7.76 (d, *J* = 8.5 Hz, 2H), 7.40 (d, *J* = 7.8 Hz, 1H), 7.30 (d, *J* = 8.4 Hz, 2H).

(E)-3-(5-(o-Tolyl)-1,3,4-oxadiazol-2-yl)acrylic acid (7b).

White powder; 64% yield (150 mg); mp 187–188°C. ^{1}H NMR (400 MHz, DMSO-d_6): δ 8.02 (d, J = 7.7 Hz, 1H), 7.46 (dp, J = 24.4, 7.6 Hz, 4H), 6.87 (d, J = 16.1 Hz, 1H), 2.64 (s, 3H).

^{13}C NMR (101 MHz, DMSO-d_6): δ 166.6, 165.4, 162.4, 138.7, 132.6, 132.5, 130.04, 129.9, 127.2, 124.8, 122.6, 22.2. HRMS (ESI, m/z): calcd for $C_{12}H_{10}N_2NaO_3$ $[M + Na]^+$ 253.0534; found 253.0541.

Biological Assays

Cell Culture for TrxR Assay

Human neuroblastoma cells (SH-SY5Y) were grown in a 1:1 mixture of Eagle's Minimum Essential Medium and F12 Medium (Sigma) supplemented with 10% fetal bovine serum (Sigma). Human glioblastoma cells (U87) were grown in Minimum Essential Medium (Sigma) containing 10% fetal bovine serum, 2 mM L-glutamine, 5000 U/mL penicillin, and 5 mg/mL streptomycin. All cell lines were obtained from the American Type Culture Collection (ATCC, Rockville, MD, USA) and were grown at 37°C in a humidified 5% CO_2 atmosphere.

Colorimetric Detection of Cell Lysate TrxR Activity

For the TrxR activity assay, lysate from SH-SY5Y cells was used. SH-SY5Y cells were washed twice with phosphate-buffered saline (PBS) and harvested from the flask with a scraper. Cells were homogenized in ice-cold 50 mM potassium phosphate buffer (pH 7.4) containing 1 mM EDTA using an Ultra Turrax T25 (Ika Werk, Janke and Kunkel Inc., Staufen, Germany). The homogenates were centrifuged at 10,000×g for 15 min at 4°C. The protein concentrations of the supernatants were determined using a Bio-Rad protein assay kit (Bio-Rad Laboratories, USA).

TrxR activity was assayed using 5,5'-dithiobis(2-nitrobenzoic acid) (DTNB, Sigma-Aldrich, USA) as the substrate [25]. The reactions were run in 96-well plates with a final volume of 100 µL in 50 mM potassium phosphate buffer (pH 7.0) containing 50 µg of cell lysate proteins, 1 mM EDTA, 50 mM KCl, 0.2 mg/mL bovine serum albumin, and 0.25 mM NADPH (Acros Organics, USA). The reaction mixture (90 µL) was incubated for 15 min on a plate shaker (PST-60HL-4, BioSan, Riga, Latvia) at room temperature with the test compounds in a concentration range of 1–200 µM. After incubation, 10 µL of DTNB was added to a final concentration of 0.5 mM. Enzyme kinetics was monitored on a TECAN Infinite M1000 PRO microplate reader by measuring the increase in absorbance at 412 nm for 20 min. The background TrxR-independent reduction of DTNB in the cell lysates, as determined in the presence of 20 µM aurothiomalate (ATM), was subtracted from each value [26, 27].

Cytotoxicity Assay

Human lung adenocarcinoma cell line H23 (ATCC #CRL-5800) and human cervix adenocarcinoma cell line HeLa (ATCC #CCL-2) from the collection of the St. Petersburg Pasteur Institute were used in the study. HeLa cell line was grown in complete α-MEM (Eagle's minimum essential medium) supplemented with 5% FBS (fetal bovine serum), penicillin, and streptomycin in a 5% CO_2 atmosphere at 36°C. H23 cell line was propagated in complete RPMI-1640 medium supplemented with 10% FBS, penicillin, and streptomycin in a 5% CO_2 atmosphere at 36°C.

Cell lines were seeded onto 96-well culture plates in the corresponding complete medium, and the plates were incubated in a 5% CO_2 atmosphere at 36°C for 24 h until formation of a cell monolayer. Test compounds were dissolved in DMSO, and serial dilutions were prepared in the corresponding serum-free maintenance medium and added to the wells containing the cell monolayer (200 µL per well, in triplicate). Intact cell control wells received 200 µL of maintenance medium with 1% DMSO. The plates were incubated for 72 h at 36°C in a 5% CO_2 atmosphere. Thereafter, the cells were observed under an inverted microscope for any signs of morphological changes, and cell viability in each well was determined using the MTT assay (tetrazolium dye reduction reaction) [28, 29].

Briefly, the wells were washed with maintenance medium, followed by the addition of 100 µL of MTT solution (3-(4,5-dimethylthiazol-2-yl)-2,5-diphenyltetrazolium bromide; 0.5 mg/mL) to each well. After incubation for 2 h at 36°C in 5% CO_2, the supernatant was removed, and the formazan crystals were dissolved in 100 µL of DMSO per well. Absorbance was measured at 540 nm using a Multiskan FC microplate reader (Thermo Scientific). The 50% cytotoxic concentration (CC_{50}), defined as the concentration causing a 50% reduction in cell viability, was calculated by regression analysis using GraphPad Prism software, version 6.01.

Molecular docking

Covalent docking was performed using ADFR 1.0 [31]. The receptor model comprised chains C and D of the 3EAN structure and two FAD molecules. Sec498 in chain C served as the covalent anchor. A Michael adduct was built for each compound before docking by defining a bond between the selenium atom of Sec498 and the β-carbon of the ligand. In the model presented here, the carboxylic acid group was neutral (COOH) and the newly formed stereocenter had the β-R configuration.

Interaction grids were calculated using AGFR 1.2rc1 [32]. Selenium was retained in the model and assigned the numerical parameters of the sulfur atom type SA. Partial charges were calculated using the sulfur analog. For each adduct, 32 genetic algorithm runs were performed, with a maximum of 10^6 scoring-function evaluations per run. The estimated binding energy of the best retained pose for each adduct was used for comparison with the experimental data.

Statistics

All *in vitro* experiments were repeated three times and primary results were analyzed using GraphPad Prism 6.01 software.

Declarations

Supplementary information

The online version of supplementary materials available at https://doi.org/10.1007/xxxxxx-xxx-xxxxx-x.

Acknowledgements

Funding

The work on the synthesis of novel compounds and the investigation of their anticancer activity was supported by the Russian Science Foundation (Project No. 25-23-20245).

Compliance with ethical standards

Conflict of interest

The authors declare no competing interests.

Publisher's note

Springer Nature remains neutral with regard to jurisdictional claims in published maps and institutional affiliations.

References

1. Zeng HH, Wang LH. Targeting Thioredoxin Reductase: Anticancer Agents and Chemopreventive Compounds. Med Chem. 2010;6:286–297. https://doi.org/10.2174/157340610793358864
2. Chupakhin EG, Krasavin MYu. Natural compounds as inhibitors of thioredoxin reductase (TrxR1). Russ Chem Bull. 2022;71(3):443–448. https://doi.org/10.1007/s11172-022-3431-4
3. Gromer S, Urig S, Becker K. The thioredoxin system—from science to clinic. Med Res Rev. 2004;24(1):40–89. https://doi.org/10.1002/med.10051
4. Peng ZF, Lan LX, Zhao F, Li J, Tan Q, Yin HW, Zeng HH. A novel thioredoxin reductase inhibitor inhibits cell growth and induces apoptosis in HL-60 and K562 cells. J Zhejiang Univ Sci B. 2008;9:16–21. https://doi.org/10.1631/jzus.b071605
5. He J, Li D, Xiong K, Ge Y, Jin H, Zhang G, Hong M, Tian Y, Yin J, Zeng H. Inhibition of thioredoxin reductase by a novel series of bis-1,2-benzisoselenazol-3(2H)-ones: Organoselenium compounds for cancer therapy. Bioorg Med Chem. 2012;20:3816–3827. https://doi.org/10.1016/j.bmc.2012.04.033

6. Li DD, He J, Zeng HH. Biological evaluation of novel selenazole-based compounds as potential thioredoxin reductase inhibitors. Appl Organomet Chem. 2012;26(11):619–624. https://doi.org/10.1002/aoc.2910
7. Santi C, Scimmi C, Sancineto L. Ebselen and Analogues: Pharmacological Properties and Synthetic Strategies for Their Preparation. Molecules. 2021;26(14):4230. https://doi.org/10.3390/molecules26144230
8. Noguchi N. Ebselen, a useful tool for understanding cellular redox biology and a promising drug candidate for use in human diseases. Arch Biochem Biophys. 2016;595:120–125. https://doi.org/10.1016/j.abb.2015.10.024
9. He L, Ji S, Lai H, Chen T. Selenadiazole derivatives as theranostic agents for simultaneous cancer chemo-/radiotherapy by targeting thioredoxin reductase. J Mater Chem B. 2015;3(42):8383–8393. https://doi.org/10.1039/c5tb01501d.
10. Chen M, Wang J, Cai F, Guo J, Qin X, Zhang H, Chen T, Ma L. Chirality-driven strong thioredoxin reductase inhibition. Biomaterials. 2024;311:122705. https://doi.org/10.1016/j.biomaterials.2024.122705
11. Wipf P, Hopkins TD, Jung JK, Rodriguez S, Birmingham A, Southwick EC, Lazo JS, Powis G. New inhibitors of the thioredoxin–thioredoxin reductase system based on a naphthoquinone spiroketal natural product lead. Bioorg Med Chem Lett. 2001;11(19):2637–2641. https://doi.org/10.1016/s0960-894x(01)00525-x
12. Zhang J, Liu Y, Shi D, Hu G, Zhang B, Li X, Liu R, Han X, Yao X, Fang J. Synthesis of naphthazarin derivatives and identification of novel thioredoxin reductase inhibitor as potential anticancer agent. Eur J Med Chem. 2017;140:564–578. https://doi.org/10.1016/j.ejmech.2017.09.027
Zuo Z, Liu X, Qian X, Zeng T, Sang N, Liu H, Zhou Y, Tao L, Zhou X, Su N, Yu Y, Chen Q, Luo Y, Zhao Y. Bifunctional Naphtho[2,3-d][1,2,3]triazole-4,9-dione Compounds Exhibit Antitumor Effects In Vitro and In Vivo by Inhibiting Dihydroorotate Dehydrogenase and Inducing Reactive Oxygen Species Production. J Med Chem. 2020;63(14):7633–7652. https://doi.org/10.1021/acs.jmedchem.0c00512
13. Qiu X, Liu Z, Shao WY, Liu X, Jing DP, Yu YJ, An LK, Huang SL, Bu XZ, Huang ZS, Gu LQ. Synthesis and evaluation of curcumin analogues as potential thioredoxin reductase inhibitors. Bioorg Med Chem. 2008;16:8035–8041. https://doi.org/10.1016/j.bmc.2008.07.054.
14. Donati C, Hashim II, Pozsoni NB, Bourda L, Hecke KV, Cazin CSJ, Visentin F, Nolan SP, Gandin V, Scattolin T. Investigation of the *in vitro* anticancer potential of bis(imino)acenaphthene–N-heterocyclic carbene transition metal complexes revealed TrxR inhibition and triggering of immunogenic cell death (ICD) for allyl palladates. RSC Med. Chem. 2025;16(6):2592–2602. https://doi.org/10.1039/d5md00039d
15. Chupakhin, E.G., Krasavin, M.Y. Natural compounds as inhibitors of thioredoxin reductase (TrxR1). Russ Chem Bull 2022;71;443–448. https://doi.org/10.1007/s11172-022-3431-4
16. Jovanović M, Zhukovsky D, Podolski-Renić A, Domraceva I, Zalubovskis R, Sencanski M, Glisic S, Sharoyko V, Tennikova T, Dar'in D, Pesic M, Krasavin M. Novel electrophilic amides amenable by the

Ugi reaction perturb thioredoxin system via thioredoxin reductase 1 (TrxR1) inhibition: Identification of DVD-445 as a new lead compound for anticancer therapy. Eur J Med Chem. 2019;181:111580. https://doi.org/10.1016/j.ejmech.2019.111580

17. Presnukhina S, Tarasenko M, Baykov S, Smirnov SN, Boyarskiy VP, Shetnev A, Korsakov MK. Entry into (E)-3-(1,2,4-oxadiazol-5-yl)acrylic acids via a one-pot ring-opening/ring-closing/retro-Diels–Alder reaction sequence. Tetrahedron Lett. 2020;61(9):151543. https://doi.org/10.1016/j.tetlet.2019.151543
18. Popov LD, Zubenko AA, Fetisov LN, Drobin YD, Klimenko AI, Bodryakov AN, Borodkin SA, Melkozerova IE. The Synthesis of (1,3,4-Oxadiazol-2-yl)Acrylic Acid Derivatives with Antibacterial and Protistocidal Activities. Russ J Bioorg Chem. 2018;44(2):238–243.https://doi.org/10.1134/S1068162018010132
19. Rozhkov SS, Ovchinnikov KL, Krasovskaya GG, Danilova AS, Kolobov AV. Synthesis of the E and Z isomers of 3-(5-aryl-1,3,4-oxadiazol-2-yl)acrylic acids. Russ J Org Chem. 2015;51(7):982–987. https://doi.org/10.1134/S1070428015070155
20. Chawla PA, Shome A, Jha KT. Hexafluorophosphate Azabenzotriazole Tetramethyl Uronium (HATU): A Unique Cross-Coupling Reagent. SynOpen. 2023;66(2). https://doi.org/10.1055/s-0042-1751499
21. Álvarez AS, Díaz-Mínguez SS, Arenas BR. Pure Appl Chem. 2024;96(5):691–707. https://doi.org/10.1515/pac-2023-1104
22. Zhang Q, Chen W, Lv X, *Weng Q, Chen M, Cui R, Liang G, Ji J*. Piperlongumine, a Novel TrxR1 Inhibitor, Induces Apoptosis in Hepatocellular Carcinoma Cells by ROS-Mediated ER Stress. Front Pharmacol. 2019;10:1180. https://doi.org/10.3389/fphar.2019.01180
23. Benmansour F, Eydoux C, Querat G, *Lamballerie X, Canard B, Alvarez K, Guillemot JK, Barral K*. Eur J Med Chem. 2016;109:146–156. https://doi.org/10.1016/j.ejmech.2015.12.046
24. Srivastava RM, Pereira MC, Faustino WWM, Coutinho K, dos Anjos JV, de Melo SJ. Synthesis, Mechanism of Formation, and Molecular Orbital Calculations of Arylamidoximes. Monatsh Chem. 2009;140:1319–1324. https://doi.org/10.1007/s00706-009-0186-7
25. Cai W, Zhang L, Song Y, Wang B, Zhang B, Cui X, Hu G, Liu Y, Wu J, Fang J. Small molecule inhibitors of mammalian thioredoxin reductase. Free Radic Biol Med. 2012;52:257–265. https://doi.org/10.1016/j.freeradbiomed.2011.10.447
26. Parrales A, McDonald P, Ottomeyer M, Roy A, Shoenen FJ, Broward M, Bruns T, Thamm DH, Weir SJ, Neville KA, Iwakuma T, Fulbright JM. Comparative oncology approach to drug repurposing in osteosarcoma. PLoS One. 2018;13:e0194224. https://doi.org/10.1371/journal.pone.0194224
27. Li H, Hu J, Wu S, Wang L, Cao X, Zhang X, Dai B, Cao M, Shao R, Zhang R, Majidi M, Ji L, Heymach JV, Wang M, Pan S, Minna J, Mehran RJ, Swisher SG, Roth JA, Fang B. Auranofin-mediated inhibition of PI3K/AKT/mTOR axis and anticancer activity in non-small cell lung cancer cells. Oncotarget. 2016;7:3548–3558. https://doi.org/10.18632/oncotarget.6516
28. Mosmann T. Rapid Colorimetric Assay for Cellular Growth and Survival: Application to Proliferation and Cytotoxicity Assays. J Immunol Methods. 1983;65:55–63. DOI: https://doi.org/10.1016/0022-

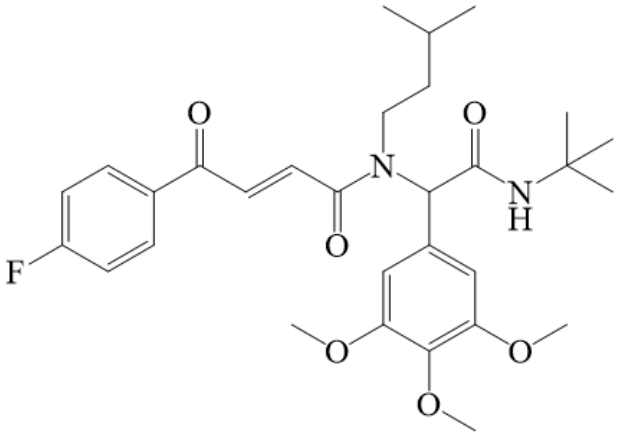
1759(83)90303-4

29. Ghasemi M, Turnbull T, Sebastian S, Kempson I. The MTT Assay: Utility, Limitations, Pitfalls, and Interpretation in Bulk and Single-Cell Analysis. Int J Mol Sci. 2021;22:12827. https://doi.org/10.3390/ijms222312827
30. Cheng Q, Sandalova T, Lindqvist Y, Arnér ESJ. Crystal structure and catalysis of the selenoprotein thioredoxin reductase 1. J Biol Chem. 2009;284(6):3998–4008. https://doi.org/10.1038/ncomms1382
31. Ravindranath PA, Forli S, Goodsell DS, Olson AJ, Sanner MF. AutoDockFR: advances in protein-ligand docking with explicitly specified binding site flexibility. PLoS Comput Biol. 2015;11(12):e1004586. https://doi.org/10.1371/journal.pcbi.1004586
32. Zhang Y, Forli S, Omelchenko A, Sanner MF. AutoGridFR: improvements on AutoDock affinity maps and associated software tools. J Comput Chem. 2019;40(32):2882–2886. https://doi.org/10.1002/jcc.26054

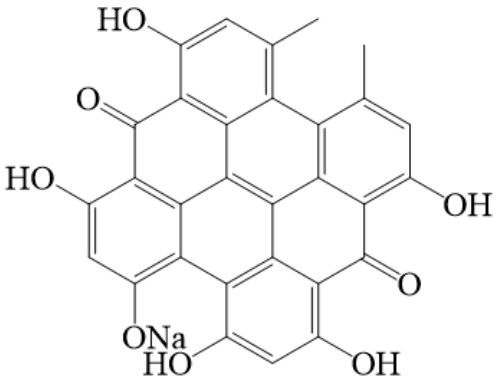
Schemes

Schemes 1 and 2 are available in the supplementary files section.

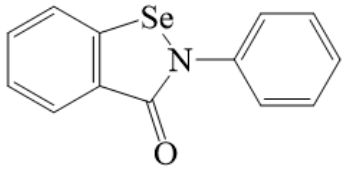
Figures



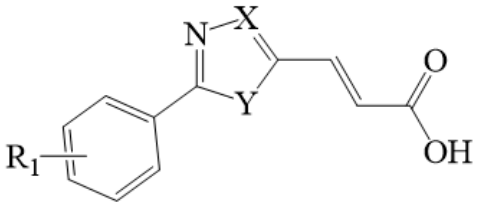
DVD-445



HYPERICIN SODIUM
Phase 3



Ebselen



This study

Figure 1

Structures of known TrxR inhibitors and the chemotype investigated in this study.

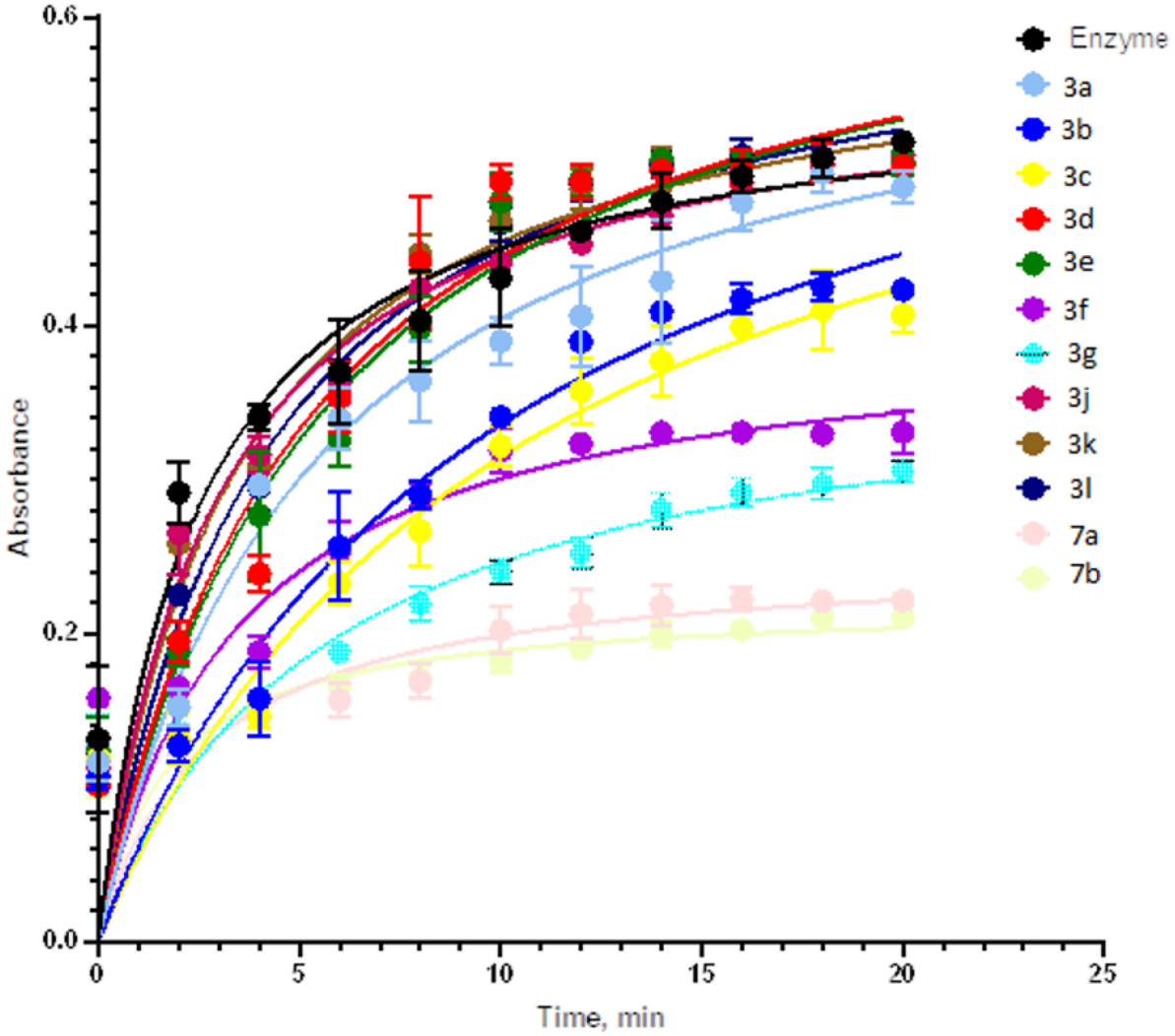


Figure 2

Figure 1. Inhibition of TrxR1 activity by oxadiazol-5-ylacrylic acid-based Michael acceptors at 25 μM.

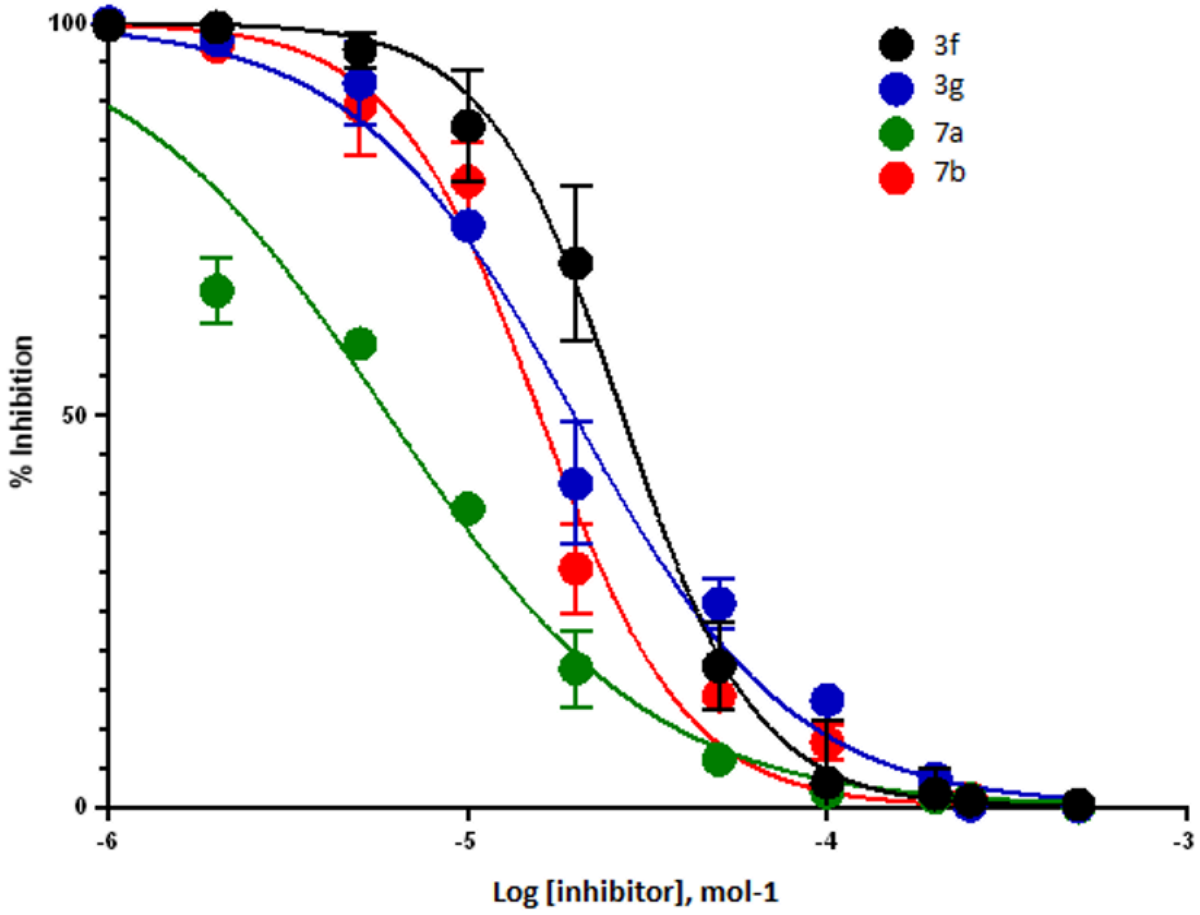


Figure 3

Figure 2. IC_{50} curves for inhibition of TrxR1 by compounds **3f**, **3g**, **7a**, and **7b** over a concentration range of 1–500 μM.

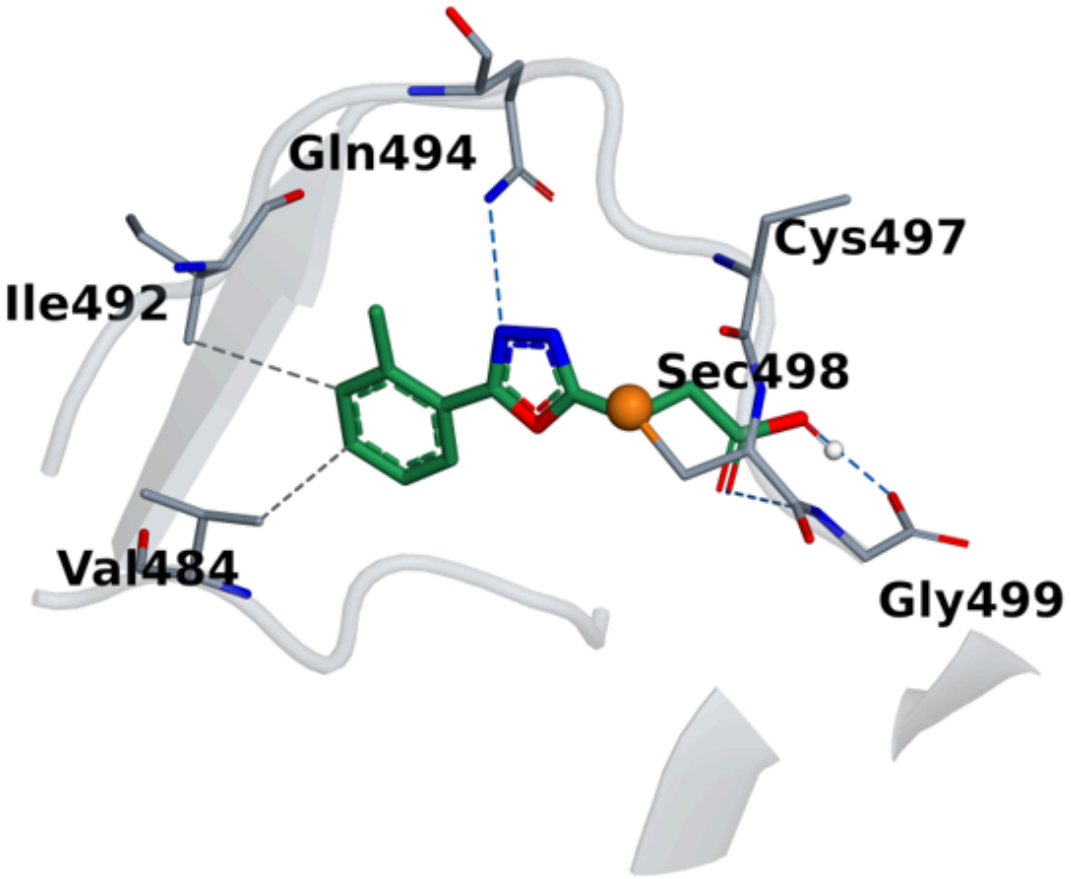


Figure 4

Figure 3. Modeled pose of the covalent adduct of compound 7b with Sec498 of rat TrxR1 in the COOH/β-R model. Blue dashed lines indicate hydrogen bonds, and gray dashed lines indicate hydrophobic contacts. The selenium atom is shown in orange. The Se–Cβ bond was specified during adduct construction and measures 1.97 Å in the retained pose.

Supplementary Files

This is a list of supplementary files associated with this preprint. Click to download.

- ESIacrylicacids05.11.docx
- GraphicalAbstract.docx
- Schemes.docx